Earth Syst. Dynam. Discuss., 2, 467–491, 2011
www.earth-syst-dynam-discuss.net/2/467/2011/
doi:10.5194/esdd-2-467-2011

Earth System Dynamics Discussions

The magnitude-timescale relationship of surface temperature feedbacks in climate models

A. Jarvis

Lancaster Environment Centre, Lancaster University, Lancaster, LA1 4YQ, UK

Received: 28 May 2011 – Accepted: 10 June 2011 – Published: 1 July 2011

Correspondence to: A. Jarvis (a.jarvis@lancs.ac.uk)

Published by Copernicus Publications on behalf of the European Geosciences Union.

Abstract

Because of the fundamental role feedbacks play in determining the characteristics of climate it is important we are able to specify both the magnitude and response timescale of the feedbacks we are interested in. This paper employs three different climate models driven to equilibrium with a 4 × CO_2 forcing to analyze the magnitude and timescales of surface temperature feedbacks. These models are a global energy balance model, an intermediate complexity climate model and a general circulation model. Rather than split surface temperature feedback into characteristic physical processes, this paper adopts a linear systems approach to split feedback according to their time constants and corresponding feedback amplitudes. The analysis reveals that there is a dominant net negative feedback realised during the first year. However, this is partially attenuated by a spectrum of positive feedbacks for time constants in the range 10 to 1000 years. This attenuation was composed of two discrete phases which are attributed to the effects of "diffusive – mixed layer" and "circulatory – deep ocean" ocean heat equilibration processes. The diffusive equilibration was associated with time constants on the decadal timescale and accounted for approximately 75 to 80 % of the overall ocean heat equilibration feedback, whilst the circulatory feedback operated on a centennial timescale and accounted for the remaining 20 to 25 % of the response. It is important to quantify these decadal and centennial feedback processes to understand the range of climate model projections on these longer timescales.

1 Introduction

Resolving global climate feedbacks has been an important feature of climate change research for many years (Hansen et al., 1984, 1985; Bony et al., 2006). Past research has tended to focus on either instantaneous or equilibrium timescale climate feedbacks given these are amenable to steady state analysis (e.g. Colman, 2003; Soden and

ESDD

2, 467–491, 2011

Magnitude-timescale relationship of surface temperature feedbacks

A. Jarvis

Held, 2006; Gregory et al., 2004; Bony et al., 2006; Forster and Taylor, 2006; Roe and Baker, 2007; Gregory and Forster, 2008; Lu and Cai, 2009). Although both of these timescales are clearly important, feedbacks in the climate system operate over a broad spectrum of timescales ranging from days to millennia (Hansen et al., 1985), and it is important that we characterise these also (Hansen et al., 2007; Knutti and Hegerl, 2008; Roe, 2009).

The timescale of climate feedbacks are determined by the dynamics of the climate system (e.g. Hoffert et al., 1980; Watts et al., 1994; Stouffer, 2004; Danabasoglu and Gent, 2009; Roe, 2009) and of ocean heat uptake in particular (Hansen et al., 1985; Watts et al., 1994; Dickinson and Schaudt, 1998). Attributing these feedbacks to specific timescales is a more difficult task than analysing the equilibrium condition given one has to accommodate the transient response of the climate system (e.g. Bates, 2007; Roe, 2009; Baker and Roe, 2009) and simple climate models have been valuable in this regard (e.g. Hansen et al., 1985; Wigley and Schlesinger, 1985; Dickinson and Schaudt, 1998; Hallegatte et al., 2006; Bates, 2007). For example, Baker and Roe (2009) investigated the effect of the oceanic heat uptake feedback on equilibrium climate sensitivity and transient climate change using a simple 1d upwelling-diffusion Global Energy Balance Model (GEBM) and showed the importance of characterising feedbacks with different timescales when inferring climate sensitivity. However, we are also interested in feedback analysis of more detailed climate system descriptions such as Earth system Models of Intermediate Complexity (EMICs) and Atmosphere-Ocean General Circulation Models (AOGCMs), and hence methods for achieving this are required (Aires and Rossow, 2003; Bates, 2007; Roe, 2009).

In this paper we present a methodology for estimating the magnitude of the contribution of feedbacks operating on the surface temperature dynamics of three different climate models, a GEBM, and EMIC and an AOGCM. Unlike previous studies that explicitly set out to differentiate surface temperature feedbacks with respect to climate *processes*, here the feedbacks will be differentiated with respect to the *timescale* of their response to surface temperature change. This is important because it will

ESDD
2, 467–491, 2011

allow an evaluation of the relative magnitudes of the *fast* and *slow* (and all intervening timescales) feedbacks operating in the climate models being studied.

2 Climate reference and feedback systems

Feedback is the generation of reference system input from its output. As a result, feedbacks can only be defined in relation to the reference system on which they operate (Stephens, 2005; Roe, 2009). We are interested in feedbacks operating to modulate the global mean surface temperature response of climate models. If ΔT (K) are annual mean global surface temperature perturbations relative to a pre-industrial baseline; Q ($\mathrm{W\,m^{-2}}$) are annual mean global energy inputs to the surface independent of ΔT (which we will call the *input forcing*); and F ($\mathrm{W\,m^{-2}}$) are annual mean global energy inputs to the surface which are dependent on ΔT (i.e. $F = f\{\Delta T\}$; which we will call the *feedback forcing*), then the global surface energy balance reference system can be described by,

$$c\,\frac{\mathrm{d}}{\mathrm{d}t}\,\Delta T = Q + F \qquad (1)$$

where c is the effective heat capacity of this element of the climate system. This heat capacity is predominately determined by the heat capacity of the well mixed surface ocean, given the land and atmosphere, to which the surface ocean is strongly coupled through large exchanges of sensible and latent heat, have relatively little thermal inertia (Dickinson and Schaudt, 1998). In defining the global surface energy balance reference system in this way we assume it to be bounded by the top of the atmosphere, across which radiant heat is exchanged with space, and by the ocean thermocline, across which sensible heat is exchanged with the deep ocean (Dickinson and Schaudt, 1998).

ESDD

2, 467–491, 2011

Magnitude-timescale relationship of surface temperature feedbacks

A. Jarvis

The physical processes giving rise to climate feedback behaviour are complex and/or nonlinear (Aires and Rossow, 2003). Rather than attempt to define these feedbacks in terms of these physical processes, which has been the subject of many studies in this area (e.g. Colman, 2003; Lu and Cai, 2009; Soden and Held, 2006), we want to try and partition the feedbacks according to the contribution of the different timescales involved in the equilibration process of climate models. This should allow an assessment of the relative importance of feedbacks being expressed on different timescales.

If we adopt a linear approach then the feedback forcing F can be considered as the sum of N feedback terms,

$$F = \sum_{i=1}^{N} F_i. \tag{2}$$

For each of these N feedbacks we can specify a timescale, to represent the speed at which the feedback equilibrates to a perturbation in ΔT, and a magnitude, to represent the contribution of the feedback to the equilibrium response of F following a perturbation in ΔT. Taking a linear systems approach, each individual feedback can be considered as a first order sub-system,

$$F_i = g_i \, \Delta T - \tau_i \frac{\mathrm{d}}{\mathrm{d}t} F_i \tag{3}$$

where τ_i (years) is the time constant or e-folding time of this feedback element measuring the timescale of its response to ΔT, and g_i ($\mathrm{W\,m^{-2}\,K^{-1}}$) is the feedback amplitude measuring the magnitude of its response to ΔT (see Fig. 1).

It will also be useful to consider the cumulative magnitude of the feedbacks experienced at timescale τ_i which is given by the feedback amplitude

$$G(\tau) = \sum_{\tau=0}^{\tau} g(\tau). \tag{4}$$

ESDD
2, 467–491, 2011

Providing the climate system is stable and fully damped, as $\tau \rightarrow \infty$ the closed-loop system described by Eqs. (1)–(3) reduces to,

$$\Delta T(\infty) = \frac{1}{-G(\infty)} Q(\infty) \quad (5)$$

and hence the equilibrium climate sensitivity, S, is given by,

$$S = \frac{1}{-G(\infty)} Q_{2\times CO_2} \quad (6)$$

where $Q_{2\times CO2}$ is the input forcing associated with a doubling in atmospheric CO_2 from a pre-industrial baseline. Hence G resembles the feedback parameters and sensitivities commonly discussed in the climate literature (e.g. Forster and Taylor, 2006). However, it is important to appreciate that G only corresponds to these more familiar feedback representation as $\tau \rightarrow \infty$ and the dynamics in the climate system have been fully extinguished. For all intermediate timescales the feedback sensitivities dF/dT and any related quantity will be highly context specific whilst G will be a stationary property of a linear dynamic system.

3 The relationship between feedback amplitudes and time constants

Because of the capacity for high order climate system models to demonstrate a broad range of dynamic behaviour one might imagine that N is large, encompassing a very broad range of values of τ. For each τ there is a corresponding value of g (and G). The aim of this study is to estimate g for every τ relevant to the equilibration of climate model ΔT given an imposed input forcing Q, i.e. we are interested in recovering the relationship $g(\tau)$ for these models. Ideally, this would be done analytically from the state equations of each model. However, analytical approaches are only possible

ESDD
2, 467–491, 2011

when analysing simple models (see Hansen et al., 1985; Roe, 2009) and are impracticable to compute for most climate models because these embrace a broad spectrum of less idealised dynamic behaviour (Prather, 1996; Roe, 2009). An alternative approach would be to exploit the range model reduction and systems identification techniques that are available for systems analysis (e.g. Goodwin and Payne, 1977; Young, 2011) which would enable the specification of highly reduced subsets of τ and g. However, given we anticipate N is large and that such methods can sometimes yield purely empirical descriptions of the system in question (Enting, 2007) we have opted for a different approach, although the results will lead us to return to this issue.

To estimate $g(\tau)$ from time series of Q and ΔT we start by pre-specifying values of τ that span the dynamic range of the model response we are investigating. Figure 2b shows the full equilibrium response of three models to the $4 \times CO_2$ forcing shown in Fig. 2a. From this we can see that the temperature response is equilibrating in <5000 years. Therefore, if we specify $\tau = 0, 10, 20, ..., 4990, 5000$ years this guarantees coverage of the dynamic response of the model because the 5000 year time constant will only have expressed 63 % of its response by then. Furthermore, a 5000 year time constant process in feedback will result in closed loop behaviour with significantly longer timescales than this. As we will see, $\tau < 1000$ years will be sufficient for all three models analysed here. A 10 year increment for τ was found to be an adequate trade off between, on the one hand capturing the subtleties of the $g(\tau)$ relationship, whilst on the other being coarse enough to make the estimation of $g(\tau)$ manageable.

Having specified τ the aim is to estimate the corresponding values of g. Despite being a quasi-linear problem (sum of linear feedback amplitudes) it is also heavily over parameterised ($N = 100$). The dynamic behaviour of a large collection of first order responses can often be represented exactly by a smaller subset of first order responses (Jarvis and Li, 2010; see later). Because of this, direct search methods for estimating $g(\tau)$, such as gradient techniques, will tend to gravitate on low order approximations and not on the 'true' $g(\tau)$ relationship (Jarvis and Li, 2011). To avoid this we have

ESDD
2, 467–491, 2011

elected to use slow cool simulated annealing to search for $g(\tau)$ because this search method is unable to exploit any covariance between the individual estimates of g and hence tends to avoid gravitating on any low order approximations.

A finite difference approximation of Eqs. (1)–(3) is used in order to vectorise the simulation so that the annealing code runs fast enough to be of utility. For this the reference system is given by,

$$\Delta T(t) = \Delta T(t-\Delta t) + \frac{\Delta t}{c}\left[Q(t) + F(t-\Delta t)\right] \tag{7a}$$

and the feedback forcings are given by,

$$F(t) = \sum_{i=1}^{N}\left[a_i F(t-\Delta t) + b_i \Delta T(t-\Delta t)\right] - 3.3\,\Delta T(t-\Delta t) \tag{7b}$$

where $g_i = b_i/(1-a_i)$ and $\tau_i = -\Delta t/\ln(a_i)$. The additional $\tau = 0$ Planck feedback of $-3.3\,\mathrm{W\,m^{-2}\,K^{-1}}$, which captures the effects of temperature driven infrared heat loss (Forster and Taylor, 2006), is stated explicitly here because, in addition to being relatively well defined, it provides a useful baseline against which all values of g_i are estimated. All results presented for $G(\tau)$ will include this feedback. The annual sample interval, Δt, used here was found to be sufficient to not introduce significant numerical errors into the finite difference approximation.

The objective of the annealing is to find the values of $g(\tau)$ that provide the least squares fit between the climate model ΔT and the output of Eq. (7). The annealing conditions found to be appropriate were 10^6 iterations and a cooling rate of 10^{-6} K per iteration. Because each annealing result has embedded in it the random perturbations of the cooling process, the results we present are the average of 100 individual anneals. This ensemble was also used as an approximate measure of the uncertainty in the $g(\tau)$ estimates. The estimation was done using the annealing algorithm in Yang et al. (2005) run in Matlab$^{\mathrm{TM}}$ 7.0, which on a 2.83 GHz Intel Core 2 Quad machine took approximately 20 h for each 100 member ensemble. These conditions were found

ESDD
2, 467–491, 2011

to provide reasonable results when recovering know synthetic $g(\tau)$ relationships, an example of which is shown in Fig. 3. It is clear from this test that there is a tendency for the method to partially smooth the estimate of $g(\tau)$ making it less peaked than it should be. This needs to be kept in mind when interpreting the results.

4 Climate models and radiative forcing runs

Because we are interested in characterising the climate model feedbacks associated with response timescales ranging from zero years right through to full equilibrium it is necessary to analyse fully equilibrated climate model perturbation runs. Such data are rare for A-OGCM's making a comprehensive intercomparison of these models not impossible at present, although as and when these data become available then clearly such an analysis could provide an informative model intercomparison exercise. In the meantime, this paper will look at three models which span a range of complexity including a GEBM (MAGICC as detailed in Eickout et al., 2004); an EMIC (UVicESCM; Weaver et al., 2001) and an A-OGCM (GFDL R15a; Manabe et al., 1991). Each of these have been driven by a 1 % annual compound CO_2 increase to $4 \times CO_2$ (taking 140 years) and then run to equilibrium. The surface temperature responses are given in Fig. 2b.

5 Results

Figure 4 shows the relationships $g(\tau)$ and $G(\tau)$ estimated for the three models. Having accounted for the Planck feedback, the values of $g(\tau)$ are positive (Fig. 4a) and, as a result, $G(\tau)$ becomes progressively less negative with increasing τ (Fig. 4b). $g(\tau)$ is at a maximum when $\tau = 0$, highlighting the importance of positive feedbacks in modulating the Planck feedback on the sub-annual timescale in these models (Bony et al., 2006; Forster and Gregory, 2006; Soden and Held, 2006). For $\tau > 0$, $g(\tau)$ remains positive

ESDD
2, 467–491, 2011

but tends to zero. The only process that is common to all three models that can explain this is the loss of ocean heat uptake from the surface as the oceans accumulate heat when equilibrating with surface temperature. Under the assumption that all $g(\tau)$ for $\tau > 0$ are attributable to this effect alone and, as $\tau \to \infty$, $g_O(\tau) \to 0$ where O denotes "ocean" feedbacks, then,

$$g_O(0) = \sum_{\tau>0}^{\infty} g(\tau) \tag{8a}$$

and,

$$G_O(\tau) = \sum_{\tau>0}^{\tau} g(\tau). \tag{8b}$$

The inset in Fig. 4b shows how $G_O(\tau)$ dissipates with increasing τ as a consequence of the ocean heat equilibration process. Baker and Roe (2009) also treated the same ocean heat equilibration process in a simple GEBM as a transient negative feedback (cf. Fig. 4b with their Fig. 6). A transient negative feedback is a negative feedback that is eroded by a series of lagged positive feedbacks, as shown in Fig. 4.

For all three models $g_O(0) \sim -1.5\,\mathrm{W\,m^{-2}\,K^{-1}}$ (see Table 1), which is approximately twice the equivalent ocean feedback parameter estimate of $-0.6\,\mathrm{W\,m^{-2}\,K^{-1}}$ presented by Gregory and Forster (2008) for the CMIP4 A-OGCM ensemble. The reason for this is provided in Fig. 4b which shows that, because the ocean heat feedback rapidly diminishes with increasing timescale, particularly for $\tau < 200$ years, the feedback amplitude estimate will be heavily dependent on the degree of equilibration in the data used in the estimation. As with the estimates of Raper et al. (2002), Gregory and Forster (2008) estimated the ocean heat uptake feedback amplitude from transient 70 year data for one percent compound CO_2 forcing experiments. Under these circumstances one would estimate something in the region of $G_O(70/e)$ which, from Fig. 4b, we can see is close to $-0.6\,\mathrm{W\,m^{-2}\,K^{-1}}$. This highlights the importance of correctly handling the dynamics in both real and model data when estimating feedback properties.

ESDD
2, 467–491, 2011

Figure 4 also shows that, after the initial stabilisation of $G(\tau)$ at $\tau \sim 200$ years, all three models reveal further increases thereafter, i.e. a secondary set of positive feedbacks are experienced (see Fig. 4a inset). This behaviour was identified by Jarvis and Li (2011) for a range of climate models looking at the feedforward dynamics of the mean surface temperature response. The cause for this behaviour can be demonstrated using the GEBM model. Like the more complex EMIC and A-OGCM, in this model surface heat is transferred to the oceans through two principal routes; "diffusion" into the near surface ocean across the thermocline, and through large scale Meridional Overturning Circulation (MOC) driving heat directly into the deep ocean from the surface (Hoffert et al., 1980). If we switch off the MOC pathway by setting the polar sinking term to zero in the GEBM we see that this abolishes the secondary long timescale peak in $g(\tau)$ (see Fig. 4a). The remaining, purely diffusive ocean heat uptake should result in an inverse relationship for $g(\tau)$ (see Kreft and Zuber, 1978) as correctly identified by the annealing results (see Fig. 4a). From this result the bi-modal relationship for $g(\tau)$ that is observed for the EMIC and the A-OGCM is understandable. The diffusive ocean heat uptake regime of the thermocline in these models gives rise to the inverse component of $g(\tau)$ for $\tau < 200$ years. The MOC heat uptake gives rise to the secondary peaked distribution in $g(\tau)$ for $\tau > 200$ years. The reason this secondary component of $g(\tau)$ is peaked is because circulatory heat distribution is tending toward (despite remaining a long way from) a well mixed process. Well mixed systems are characterised by a single timescale and feedback amplitude i.e. are they infinitely peaked in $g(\tau)$. Therefore, poorly mixed systems such as the global deep oceans, which have a blend of both diffusive and circulatory distribution mechanisms, produce a peaked distribution of feedback amplitudes with timescale. An alternative but related way of accounting for the $g(\tau)$ distribution of the deep ocean is to consider the surface as being linked to a very large number of deep ocean water bodies. Each of these is connected to the surface in different ways depending on the circulatory architecture of the ocean. This is equivalent to there being a distribution of values of g and τ to describe the connectivity between these water bodies and the surface, with the first moment of this distribution

ESDD
2, 467–491, 2011

describing the most common degree of connectivity. It is important to keep in mind that the annealing method does have a tendency to smooth the peak in $g(\tau)$ (see Fig. 3) and, therefore, it is likely to be slightly more peaked than shown in Fig. 3.

For all three models these long timescale adjustments to the oceanic feedback amount to the preservation of a feedback amplitude of approximately $-0.35\,\mathrm{W\,m^{-2}\,K^{-1}}$ up until the equilibration of this process. We see from Fig. 4 that this secondary equilibration starts at around $\tau \sim 200$ years and finishes at $\tau \sim 400$ years for the EMIC, whilst for the AOGCM model this processes occurs some 200 years later. Stouffer (2004) plots the spatial distribution of the times taken to achieve either 30 or 70 % equilibration of ocean temperature in the same A-OGCM, but run under $2 \times CO_2$ forcing. The 30 % timescale ranges from 100 to 900 years whilst the 70 % timescale ranges from 100 to 1800 years. It would be tempting to try and relate these spatial distributions to the results shown in Fig. 3. However, it is not clear at this stage how to map Stouffer's (2004) results into feedbacks experienced at the surface and hence $g(\tau)$.

Because $G(0) = -3.3 + g_O(0) + g_A(0)$, where $g_A(0)$ is the instantaneous net atmospheric feedback amplitude, it is possible to estimate $g_A(0)$ because $g_O(0)$ is known. The results for the three models are given in Table 1 and show relatively little difference between the three models with $g_A(0) \sim 2.3\,\mathrm{W\,m^{-2}\,K^{-1}}$. This estimate is indistinguishable from the estimate of $2.2 \pm 0.26\,\mathrm{W\,m^{-2}\,K^{-1}}$ for the same quantity made by Colman (2003) for a suite of A-OGCM's by summing individual estimates of the water vapour, cloud, albedo, and lapse rate feedback parameters. This again provides a degree of independent verification of the annealing results. The GEBM has no explicit representation for $g_A(0)$ and hence its behaviour in this regard is a result of an implicit parameterization. This is not surprising given GEBM's including MAGICC are tuned to emulate A-OGCM's (Raper et al., 2002). For reference, Fig. 2b shows the outgoing longwave forcing $F_A = (-3.3 + g_A(0))\Delta T$ for all three models.

Table 1 also shows the estimated values of the surface heat capacity c and equivalent 1d well-mixed ocean depths of the three models. This is significantly larger in the GEBM due to having a parameterisation for ocean heat uptake that allows for

ESDD
2, 467–491, 2011

Magnitude-timescale relationship of surface temperature feedbacks

A. Jarvis

the effective downward penetration of the mixed layer into the thermocline with time (Hansen et al., 1985; Watterson, 2000), meaning this extends well beyond the 90 m specified in this model. In contrast, the surface heat capacity of the EMIC and AOGCM are much closer to that expected for the real world surface mixed layer with equivalent depths of 74 and 34 m respectively, implying a somewhat more realistic representation of the coupling between the surface and lower ocean.

6 Implications for simple models

An important consequence of the bi-modal character of $g(\tau)$ shown in Fig. 4a is that this suggests reduced order forms of these climate models which could provide valuable summaries of the core dynamic characteristics of surface energy balance. This reduction in model order stems from the fact that, providing they are either low variance or symmetric, the dynamics produced by distributions of first order processes such as those shown in Fig. 4a can be accurately represented by the first moment of these distributions (Jarvis and Li, 2011). Given we have two such distributions then, taking into account the reference system, a reduced third order model is implied. Third order analogues of the climate system energy balance have been proposed previously (e.g. Dickinson, 1981; Greiser and Schonweis, 2001; Li and Jarvis, 2009). However, here we will define the structure and parameterisation directly from the feedback analysis results.

Figure 4 suggests one atmospheric and two transient ocean heat feedbacks operating on the reference system i.e.,

$$c\,\frac{d}{dt}\,\Delta T = Q - F_A - F_D - F_C \tag{9}$$

where $F_A = (3.3 - g_A)\Delta T$ is the "atmospheric" feedback forcing; $F_D = g_C(\Delta T - \Delta T_C)$ is the (diffusive) ocean heat uptake and $F_O = g_O(\Delta T - \Delta T_O)$ is the (circulatory) ocean heat uptake. This structure differs from the usual layer cascade box models (Dickinson, 1981; Greiser and Schonweis, 2001; Hooss, 2001; Li and Jarvis, 2009) because the two ocean heat reservoirs interact directly with the ocean mixed layer. g_C are both the ocean heat exchange efficiencies and the feedback amplitudes of these two processes. From this we get,

$$c\,\frac{\mathrm{d}}{\mathrm{d}t}\,\Delta T(t) = Q(t) + \boldsymbol{g}_\mathrm{R}\,\Delta T(t) + g_\mathrm{D}\,\Delta T_\mathrm{D}(t) + g_\mathrm{C}\,\Delta T_\mathrm{C}(t) \tag{10a}$$

$$\tau_\mathrm{D,C}\,\frac{\mathrm{d}}{\mathrm{d}t}\,\Delta T_\mathrm{D,C}(t) = g_\mathrm{D,C}\,\Delta T(t) - \Delta T_\mathrm{D,C}(t) \tag{10b}$$

where $\boldsymbol{g}_\mathrm{R} = -3.3 + g_\mathrm{A} - g_\mathrm{D} - g_\mathrm{C}$ i.e. all $\tau = 0$ feedback terms aggregate in the reference system. It is tempting to formulate Eq. (10b) in the form of Eq. (10a) by specifying heat capacities for the two oceanic responses. We will avoid this because, as with the mixed layer, this would imply the temperature states $\Delta T_\mathrm{D,C}$ represent well-mixed conditions. Clearly this is not so and, were we to do this, the implied heat capacities would be significantly less than that known to reside in the parent models (Grieser and Schönwiese, 2001). Instead, we have retained $\tau_\mathrm{D,C}$ to describe the average dynamic timescale over which the ocean heat equilibrations occur.

The parameters for Eq. (10) for the three climate models are given in Table 1. In each case the reduced order models are able to explain more than 99.9 % of the variance of their higher order parents. The values of τ_D are comparable amongst the three models whereas the value of τ_C is significantly smaller for the EMIC. The values of $g_\mathrm{D,C}$ do not depend on the structure of Eq. (10) because they are simply the areas under the two distributions shown in Fig. 4a for $\tau > 0$. As a result, these values should be representative of the actual efficiencies of heat exchange with the diffusive and circulatory ocean regimes in these models. The values of $g_\mathrm{D,C}$ shown in Table 1 are comparable between the three models, although g_C is smaller in the A-OGCM consistent with the finding that the 4 × CO_2 forcing of this model was associated with significant weakening of MOC (Manabe et al., 1991). The ratio $g_\mathrm{D,C}/(g_\mathrm{D} + g_\mathrm{C})$ is a measure of the relative importance of the two ocean heat uptake pathways in the ocean heat uptake feedback.

ESDD
2, 467–491, 2011

From the values in Table 1 this partitioning is approximately 3:1 diffusive:circulatory for the GEBM and EMIC models and 4:1 for the AOGCM, demonstrating the decadal timescale "diffusive" heat loss pathway is significantly more important in affecting the reference system energy balance dynamics in these three models. Because the MOC heat uptake pathway appears less important for determining the dynamics of the surface temperature response, whilst also being very uncertain, this suggest that dropping this term from simple climate models would not radically impact on model performance, particularly for timescales <200 years.

7 Discussion and conclusion

Such a small sample of climate models is not intended to reflect the diversity of climate model behaviour. This sample was determined by the desire to represent a spectrum of climate model types and the rarity of full equilibrium run A-OGCM data sets. The analysis presented demonstrates how the magnitude of feedbacks are related to their response timescale in these models. This relationship has three general traits. Firstly, it is comprised of a large net negative feedback at zero lag comprised of outgoing long wave and ocean heat uptake effects which are partially offset by instantaneous atmospheric adjustment. As feedback response timescale increases, this net negative feedback is attenuated by a series of positive feedbacks which we argue are attributable to the equilibration of heat between the surface and the oceans. This equilibration process appears to be divisible into two discrete components; a decadal timescale equilibration which relates to diffusive ocean heat uptake, accounting for approximately 75 to 80 percent of the total equilibration dynamic; and a century timescale equilibration which relates to the large scale circulation of heat into the oceans, accounting for the remaining 20 to 25 %. To see if the results presented here are more general obviously requires more full equilibrium run data sets becoming available. Because ocean circulation can depend on the nature of the forcing applied to A-OGCM's (Manabe et al., 1991; Stouffer, 2004) $g(\tau)$ can be a function of the forcing disturbance,

ESDD
2, 467–491, 2011

making any generalisation more difficult. It must be stressed that this is because the underlying dynamics of the A-OGCM are changing and not because the estimates of the feedback amplitudes are biased by using a static analysis framework on a dynamic system (see e.g. Gregory et al., 2004).

The results from the feedback magnitude-timescale analysis highlight that the link between simple linear (box and impulse response) climate models and their complex counterparts is not as superficial as originally believed. This link is partly explained by the fact that imperfect mixing processes in the ocean can still have a characteristic time constants and amplitudes, hence the peak in $g(\tau)$. Imperfect mixing is analogous to perfect mixing occurring within a fraction of the control volume (Beer and Young, 1983). As a result, the ratio of the actual control volume to that estimated for an appropriate box model analogue could provide a useful measure of the degree of ocean mixing in play. As with most box model analogues of the global energy balance, if $c_{\mathrm{D,C}} = \tau_{\mathrm{D,C}}/g_{\mathrm{D,C}}$, then parameter values in Table 1 give rise to approximately one quarter of the heat capacity known to reside in the global oceans.

Aires and Rossow (2003) rightly highlight a range of limitations of adopting a linear feedback approach for characterising feedback processes, and in particular the inappropriate accounting for interactions between feedback processes the linear additive framework provides. In principle, the linear systems approach need not be restricted to additive feedbacks and could also consider a range of configurations of first order systems which map to physical processes (see e.g. Li et al., 2009 for a global carbon cycle example). However, this would require relatively detailed knowledge of the 3-D architecture of the global energy balance system. This is why the analysis presented here was initially restricted to identifying the magnitude of feedbacks operating on particular timescales, with the interpretation in terms of processes only coming in light of the results. Therefore, the main limitation of the current approach is not the additive structure of the feedbacks, but rather the assumed time invariance of the feedback amplitudes. For example, it is clear from Manabe et al. (1991) that the $4 \times CO_2$ A-OGCM run analysed here has non-stationary ocean circulation which would equate

ESDD
2, 467–491, 2011

to a degree of nonstationarity in $g(\tau)$. That said, it is remarkable how well linear frameworks like this perform when accounting for A-OGCM behaviour (see also Gregory et al., 2004; Forster and Taylor, 2006; Li and Jarvis, 2009). Two candidate mechanisms for giving rise to this are the nature of the network connections within these models and the overall balance of negative over positive feedback. Further research on these traits is needed.

Acknowledgements. I would like to thank, David Leedal, Paul Smith, Arun Chotai and Sile Li for valuable discussions had during the development of the analysis and Peter Young for ongoing discussions on climate model dynamics. I also express my gratitude to Michael Eby, Gokhan Danabasoglu and Ronald Stouffer who kindly provided the equilibrated climate model data. This paper has benefitted significantly from the comments of two anonymous reviewers and the editorial guidance of Piers Forster.

References

Aires, F. and Rossow, W. B.: Inferring instantaneous, multivariate and nonlinear sensitivities for the analysis of feedback processes in a dynamical system: Lorenz model case-study, Q. J. Roy. Meteorol. Soc., 129, 239–275, 2003.

Barker, M. B. and Roe, G. H.: The shape of things to come: why is climate change so unpredictable?, J. Climate, 22, 4574–4589, doi:10.1175/2009JCLI2647.1, 2009.

Bates, J. R.: Some considerations of the concept of climate feedback, Q. J. Roy. Meteorol. Soc., 133, 545–560, 2007.

Beer, T. and Young, P. C.: Longitudinal dispersion in natural streams, American Society of Civil Engineering, J. Environ. Eng.-ASCE, 109, 1049–1067, 1983.

Bony, S., Colman, R., Kattsov, V. M., Allan, R. P., Bretherton, C. S., Dufresne, J.-L., Hall, A., Hallegatte, S., Holland, M. M., Ingram, W., Randall, D. A., Soden, B. J., Tselioudis, G., and Webb, M. J.: How well do we understand and evaluate climate change feedback processes?, J. Climate, 19, 3445–3482, 2006.

Colman, R. A.: A comparison of climate feedbacks in general circulation models, Clim. Dynam., 20, 865–873, 2003.

Danabasoglu, G. and Gent, P. R.: Equilibrium climate sensitivity: is it accurate to use a slab ocean model?, J. Climate, 22, 2494–2499, 2009.
Dickinson, R. E.: Convergence Rate and Stability of Ocean-Atmosphere Coupling Schemes with a Zero-Dimensional Climate Model, J. Atmos. Sci., 38, 2112–2120, 1981.
Dickinson, R. E. and Schaudt, K. J.: Analysis of timescales of response of a simple climate model, J. Climate, 11, 97–106, 1998.
Eickhout, B., den Elzen, M. G. J., and Kreileman, G. J. J.: The Atmosphere-Ocean System of IMAGE 2.2, A global model approach for atmospheric concentrations, and climate and sea level projections, RIVM report 481508017/2004, RIVM, Bilthoven, 2004.
Enting, I. G.: Laplace transform analysis of the carbon cycle, Environ. Model. Softw., 22, 1488–1497, 2007.
Forster, P. M. and Taylor, K. E.: Climate Forcings and Climate Sensitivities Diagnosed from Coupled Climate Model Integrations, J. Climate, 19, 6181–6194, 2006.
Goodwin, G. C. and Payne, R. L.: Dynamic System Identification: Experiment Design and Data Analysis, Academic Press, London, 1977.
Gregory, J. M. and Forster, P. M.: Transient climate response estimated from radiative forcing and observed temperature change, J. Geophys. Res., 113, D23105, doi:10.1029/2008JD010405, 2008.
Gregory, J. M., Ingram, W. J., Palmer, M. A., Jones, G. S., Stott, P. A., Thorpe, R. B., Lowe, J. A., Johns, T. C., and Williams, K. D.: A new method for diagnosing radiative forcing and climate sensitivity, Geophys. Res. Lett., 31, L03205, doi:10.1029/2003GL018747, 2004.
Grieser, J. and Schönwiese, C.-D.: Process, forcing, and signal analysis of global mean temperature variations by means of a three-box energy balance model, Climatic Change, 48, 617–646, 2001.
Hallegatte, S., Lahellec, A., and Grandpeix, J. Y.: An elicitation of the dynamic nature of water vapor feedback in climate change using a 1D model, J. Atmos. Sci., 63, 1878–1894, 2006.
Hansen, J. E., Lacis, A., Rind, D., Russell, G., Stone, P., Fung, I., Ruedy, R., and Lerner, J.: Climate sensitivity: analysis of feedback mechanisms, in: Climate Processes and Climate Sensitivity, edited by: Hansen, J. E. and Takahashi, T., American Geophysical Union, Washington, DC, USA, 130–163, 1984.
Hansen, J., Russell, G., Lacis, A., Fung, I., Rind, D., and Stone, P.: Climate response times: Dependence on climate sensitivity and ocean mixing, Science, 229, 857–859, 1985.

ESDD
2, 467–491, 2011

Hansen, J., Sato, M., Kharecha, P., Russell, G., Lea, D. W., and Siddall, M.: Climate change and trace gases, Philos. T. Roy. Soc. A, 365, 1925–1954, 2007.
Hoffert, M. I., Calligari, A. J., and Hseich, C.-T.: The role of deep sea heat storage in the secular response to climate forcing, J. Geophys. Res., 85, 6667–6679, 1980.
Hooss, G.: Aggregate models of climate change: developments and applications, PhD thesis, Max-Planck-Institute for Meteorology, Hamburg, Germany, 2001.
Jarvis, A. J. and Li, S.: On the timescale-gain relationship of climate models, Clim. Dynam., 36, 523–531, doi:10.1007/s00382-010-0753-y, 2011.
Knutti, R. and Hegerl, G. C.: The equilibrium sensitivity of the Earth's temperature to radiation change, Nat. Geosci., 1, 735–743, 2008.
Kreft, A. and Zuber, A.: On the physical meaning of the dispersion equation andits solutions for different initial and boundary conditions, Chem. Eng. Sci., 33, 1472–1480, 1978.
Li, S. and Jarvis, A. J.: The global mean surface temperature dynamics of an AOGCM: The HadCM3 4 × CO_2 forcing experiment revisited, Clim. Dynam., 33, 817–825, doi:10.1007/s00382-009-0581-0, 2009.
Li, S., Jarvis, A. J., and Leedal, D. T.: Are response function representations of the global carbon cycle ever interpretable?, Tellus B, 61, 361–371, 2009.
Lu, J. and Cai, M.: A new framework for isolating individual feedback processes in coupled general circulation climate models, Part I: formulation, Clim. Dynam., 32, 873–885, 2009.
Manabe, S., Stouffer, R. J., Spelman, M. J., and Bryan, K.: Transient responses of a coupled ocean-atmosphere model to gradual changes of atmospheric CO_2, Part I. Annual mean response, J. Climate, 4, 785–817, 1991.
Prather, M. J.: Time scales in atmospheric chemistry: Theory, GWPs for CH_4 and CO, and runaway growth, Geophys. Res. Lett., 23, 2597–2600, 1996.
Raper, S. C. B., Gregory, J. M., Stouffer, R. J.: The role of climate sensitivity and ocean heat uptake on AOGCM transient temperature response, J. Climate, 15, 124–130, 2002.
Roe, G. H.: Feedbacks, timescales and seeing red, Ann. Rev. Earth Planet. Sc., 37, 93–115, 2009.
Roe, G. H. and Barker, M. B.: Why is climate sensitivity so unpredictable?, Science, 318, 629–632, 2007.
Soden, B. J. and Held, I. M.: An assessment of climate feedbacks in coupled ocean-atmosphere models, J. Climate, 19, 3354–3360, 2006.

Stephens, G. L.: Cloud Feedbacks in the Climate System: A Critical Review, J. Climate, 18, 237–273, 2005.
Stouffer, R. J.: Time scales of climate response, J. Climate, 17, 209–217, 2004.
Watterson, I. G.: Interpretation of simulated global warming using a simple model, J. Climate, 13, 202–215, 2000.
Watts, R. G., Morantine, M. C., and Achutarao, K.: Timescales in energy balance climate models, 1. The limiting case solutions, J. Geophys. Res., 99, 3631–3641, 1994.
Weaver, A. J.: The UVic Earth System Climate Model: Model description, climatology and application to past, present and future climates, Atmos. Ocean, 39(3), 361–428, 2001.
Wigley, T. M. L. and Schlesinger, M. E.: Analytical solution for the effect on increasing CO_2 on global mean temperature, Nature, 315, 649–652, 1985.
Yang, W. Y., Cao, W., Chung, T.-S., and Morris, J.: Applied numerical method using MATLAB®. Wiley-Interscience, New Jersy, 2005.
Young, P. C.: Recursive Estimation and Time-Series Analysis, Springer-Verlag, Berlin, 2011.

ESDD
2, 467–491, 2011

Magnitude-timescale relationship of surface temperature feedbacks

A. Jarvis

Table 1. Estimates of various parameters derived from the relationships shown in Fig. 4 (see text for explanation). The values of $\tau_{D,C}$ are the median values of the distributions shown in Fig. 3a and $g_{D,C}$ are the areas under the distribution function. Note, $-g_O(0) = g_D + g_C$. The 95 % confidence intervals are derived from the 100 member ensemble of the simulated annealing results.

Model	c, h ($\mathrm{W\,m^{-2}\,K^{-1}\,a^{-1}}$) (m)	5th, 95th percentiles	$g_O(0)$, $g_A(0)$ ($\mathrm{W\,m^{-2}\,K^{-1}}$)	5th, 95th percentiles	τ_R, τ_D, τ_C (years)	5th, 95th percentiles	g_R, g_D, g_C ($\mathrm{W\,m^{-2}\,K^{-1}}$)	5th, 95th percentiles
MAGICC ($\pi = 0.4$)	21.93 168.95	10.57, 32.91 81.43, 253.54	−1.52 2.30	−0.94, −2.09 1.73, 2.89	8.70 20 500	3.57, 16.69 – –	−2.52 1.13 0.39	−3.09, −1.94 0.50, 1.71 0.29, 0.45
MAGICC ($\pi = 0.0$)	18.67 143.83	9.60, 27.48 73.96, 211.71	−1.55 2.30	−1.03, −2.05 1.81 2.83	–	–	–	–
UVicESCM	9.59 73.88	2.22, 17.42 17.10, 134.20	−1.55 2.27	−1.08, −2.04 1.79, 2.74	3.72 20 300	0.75–8.26 – –	−2.58 1.14 0.41	−3.06, −2.11 0.60, 1.63 0.33, 0.51
GFDLR15a	4.35 33.51	1.67, 9.28 12.87, 71.49	−1.49 2.37	−1.06, −2.01 1.84, 2.79	1.80 485 15	0.58, 4.58 – –	−2.42 1.19 0.30	−2.94, −2.00 0.78, 1.69 0.22–0.35

Discussion Paper | Discussion Paper | Discussion Paper | Discussion Paper |

ESDD
2, 467–491, 2011

Magnitude-timescale relationship of surface temperature feedbacks

A. Jarvis

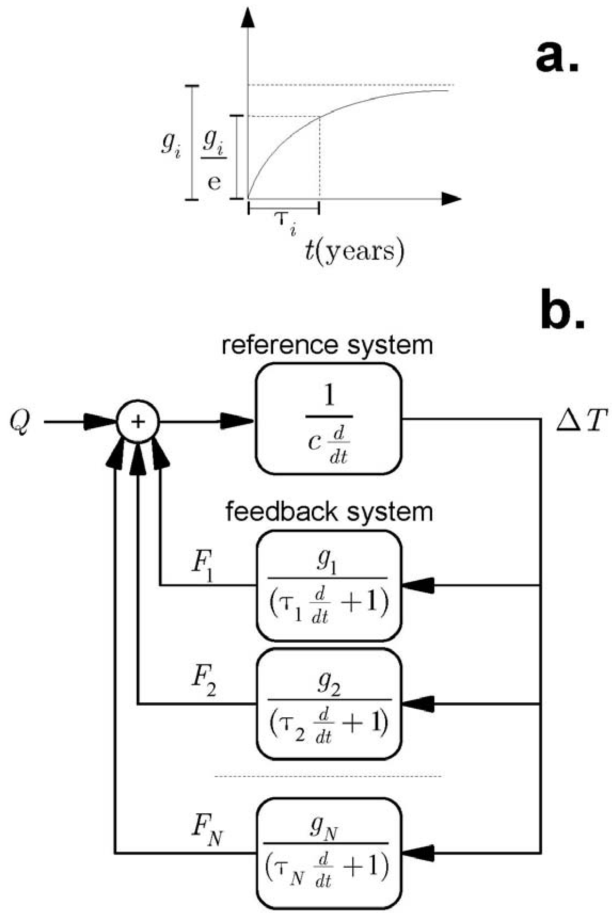

Fig. 1. (a) The generic response of the first order feedback elements shown in **(b)**, showing the time constant τ in relation to its feedback amplitude g.

ESDD
2, 467–491, 2011

Magnitude-timescale relationship of surface temperature feedbacks

A. Jarvis

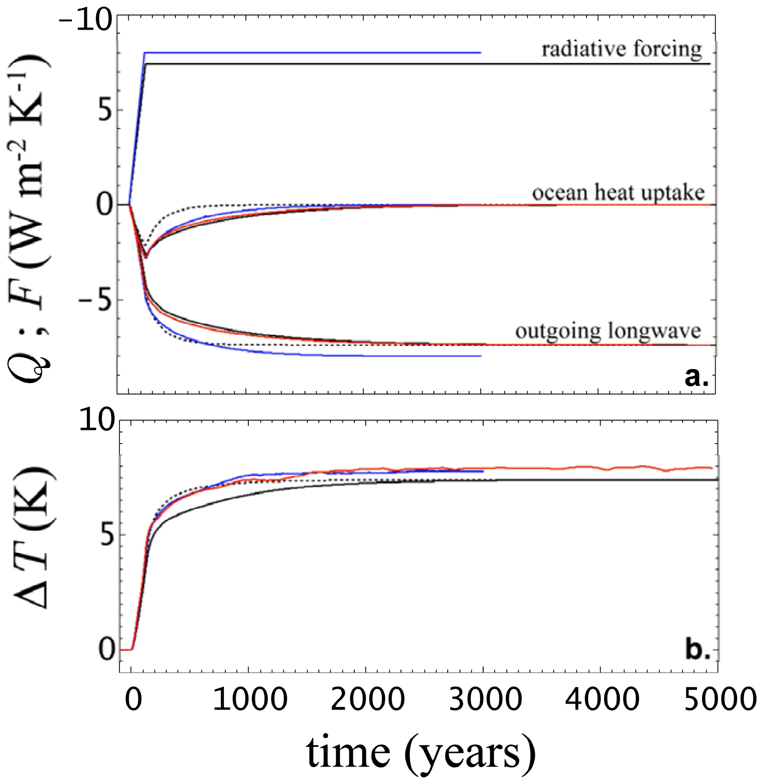

Fig. 2. **(a)** The radiative forcings, ocean heat uptake and outgoing long wave radiative heat fluxes associated with the temperature perturbations shown in **(b)** (see text). The radiative forcings marked black are common to both the GEBM and AOGCM model runs. **(b)** The global surface temperature response of three climate models to the radiative forcings shown in **(a)**: MAGICC-GEBM with (black) and without (black-dashed) polar sinking; UVicESCM-EMIC (blue); GFDLR15a-AOGCM (red).

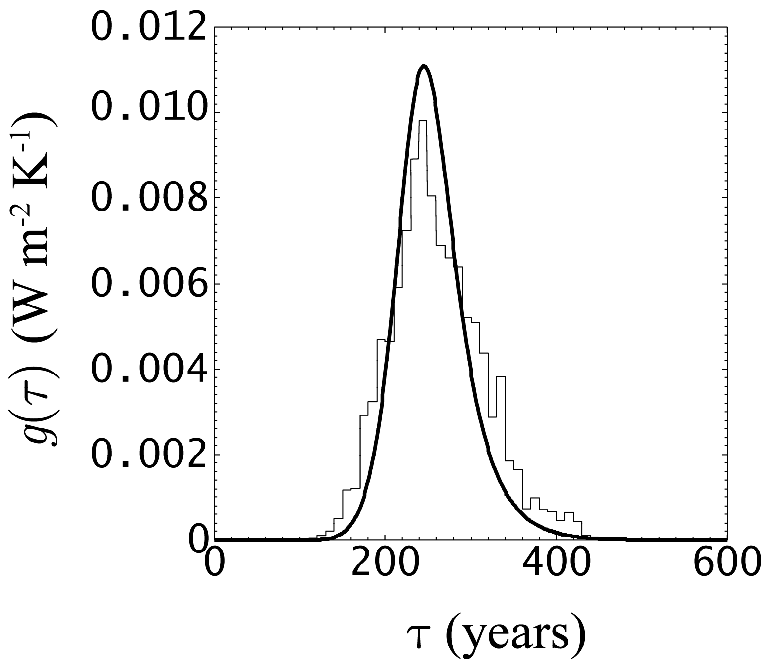

Fig. 3. The relationship between feedback amplitude, g, and its corresponding time constant τ for a synthetic test case. The thick line has been used to generate a unit step response to which the structure in Fig. 1 has been optimised using the simulated annealing methodology outlined in the text. The thin line is the resultant estimate of the same relationship.

ESDD
2, 467–491, 2011

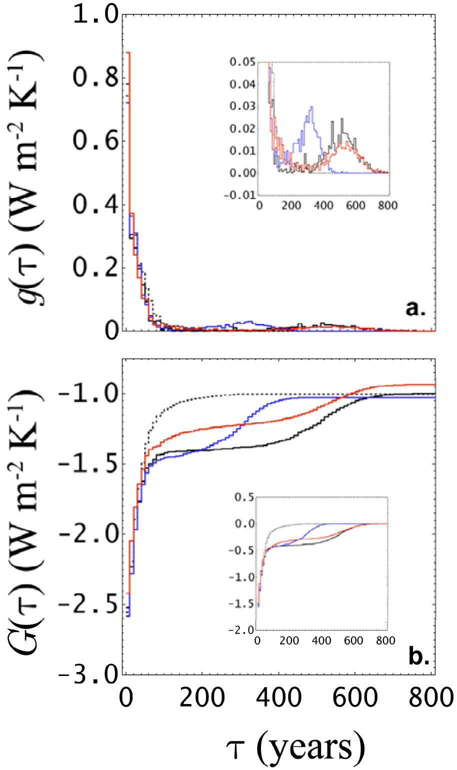

Fig. 4. (a) The relationship between feedback amplitude g and time constant τ estimated from the data shown in Fig. 2: MAGICC-GEBM with (black) and without (black-dashed) polar sinking; UVicESCM-EMIC (blue); GFDLR15a-AOGCM (red). The inset shows the tail of the relationship in more detail. **(b)** The relationship between the cumulative feedback amplitude G and τ here $G(\tau) = \sum_{\tau=0}^{\tau} g(\tau) - 3.3$. The inset shows the cumulative ocean heat uptake feedback amplitude G_O (see text).

ESDD
2, 467–491, 2011

Magnitude-timescale relationship of surface temperature feedbacks

A. Jarvis